University of Bath

Towards an Understanding of Molecule Capture by the Antennae of Male Beetles Belonging to the Genus *Rhipicera* (Coleoptera, Rhipiceridae)

Andrew Ramsey,[1] Terry F. Houston,[2] Alexander D. Ball,[3] Tomasz Goral,[3] Maxwell V. L. Barclay,[4] and Jonathan P. L. Cox[5*]

[1]Nikon Metrology, Icknield Way, Tring, Hertfordshire HP23 4JX, UK

[2]Department of Terrestrial Zoology, Western Australian Museum, 49 Kew Street, Welshpool, Western Australia 6986, Australia

[3]Department of Science Facilities, Natural History Museum, Cromwell Road, London SW7 5BD, UK

[4]Department of Life Sciences, Natural History Museum, Cromwell Road, London SW7 5BD, UK

[5]Department of Chemistry, University of Bath, Bath BA2 7AY, UK

[*]Correspondence to: Jonathan P. L. Cox, Department of Chemistry, University of Bath, Bath BA2 7AY, UK. Tel.: +44 1225 386548; Fax: +44 1225 386231. E-mail: j.p.l.cox@bath.ac.uk.

Running title: Olfactory influences in *Rhipicera* beetles

ABSTRACT

Working on the hypothesis that an important function of the lamellate antennae of adult male beetles belonging to the genus *Rhipicera* is to detect scent associated with female conspecifics, and using field observations, anatomical models derived from X-ray microcomputed tomography, and scanning electron microscopy, we have investigated the behavioural, morphological, and morphometric factors that may influence molecule capture by these antennae. We found that male beetles fly upwind in a zigzag manner, or face upwind when perching, behaviour consistent with an animal that is tracking scent. Furthermore, the ultrastructure of the male and female antennae, like their gross morphology, is sexually dimorphic, with male antennae possessing many more of a particular type of receptor - the sensillum placodeum - than their female counterparts (approximately 30,000 *v.* 100 per antenna, respectively). Based on this disparity, we assume that the sensilla placodea on the male antennae are responsible for detecting scent associated with female *Rhipicera* beetles. Molecule capture by male antennae in their alert, fanned states is likely to be favoured by: a) male beetles adopting prominent, upright positions on high points when searching for scent; b) the partitioning of antennae into many small segments; c) antennal morphometry (height, width, outline area, total surface area, leakiness, and narrow channels); d) the location of the sensilla placodea where they are most likely to encounter odorant molecules; and e) well dispersed sensilla placodea. The molecule-capturing ability of male *Rhipicera* antennae may be similar to that of the pectinate antennae of certain male moths.

Keywords: Anatomical reconstruction; *Antheraea*; *Bombyx*; insect; olfaction

INTRODUCTION

Some insects have elaborate antennae for detecting trace quantities of airborne odorant molecules. The male silk moth, *Bombyx mori* (Lepidoptera, Bombycidae), whose pectinate (comb-like) antennae can detect as few as 3,000 molecules of female pheromone per millilitre of air, is a classic example (for reviews, see Kaissling, 2009, 2014). Understanding the first event in signal detection – transport of odorant molecules to the antennal surface – is important not only because this event is part of a fundamental biological process (olfaction), but also because the lessons learnt could be applied to improving the sensitivity of artificial sensory systems.

Transport of airborne odorant molecules to the antennal surface ('molecule capture'; Koehl, 2006; Kaissling, 2009) involves two steps. In the first, the odorant molecules are brought into proximity of the antennal surface by convection (i.e. the bulk movement of air, which could be generated by, for example, the wind, or by the insect flying; Denny, 1993). In the second step, the odorant molecules must diffuse from the air to the antennal surface (Vogel, 1994). Note that diffusion cannot govern the entire transport process, because diffusion times in air, even over relatively short distances, are long (Denny, 1993, Fig. 6.3). Factors that can influence molecule capture include the behaviour of the insect (e.g. wing fanning in male *B. mori*; Loudon and Koehl, 2000), the geometry of the antennae (Kaissling, 1971), the morphometry of the sensory surface (e.g. the quantity of a substance diffused to a surface is proportional to the area of that surface; LaBarbera and Vogel, 1982; Schmidt-Nielsen, 1997), the boundary layer formed when air moves over an object (e.g. the ground, or an insect's body; Sutton, 1949; Schneider et al., 1998), and the number and distribution of the olfactory receptors on the sensory surface (Chapman, 1982; Kanaujia and Kaissling, 1985; Berg and Purcell, 1977; Berg, 1983).

We have chosen to study molecule capture by the antennae of male beetles belonging to the genus *Rhipicera* (Coleoptera, Rhipiceridae). Five species are currently recognised in this genus (Jin et al., 2013). Based on morphological characters, all five species are closely related (e.g. Jin et al., 2013, Table 1). Precisely how they are related to each other is not, however, known (e.g. there are no molecular data). All five species have been recorded only in Australia (Jin et al., 2013). Very little is known about their biology (Lawrence, 2005; Jin et al., 2013).

3

There were three reasons for choosing to study molecule capture in *Rhipicera* beetles. First, there are no previous studies of molecule capture by the antennae of beetles. Second, the antennae of beetles in the genus *Rhipicera* are sexually dimorphic (Jin et al., 2013, Fig. 3): the size and shape of the male antennae (Fig. 1) suggest that these antennae may be involved in detecting trace quantities of odorant molecules associated with female conspecifics[1]. This suggestion is based on: a) the fact that the antennae will have a relatively large surface area, encouraging diffusion of odorant molecules to the antennal surface (LaBarbera and Vogel, 1982; Schmidt-Nielsen, 1997); b) the assumption that many sensilla (the sensory structures on the antennal surface; Schneider, 1964; Altner, 1977; Altner and Prillinger, 1980) can be accommodated on the relatively large surface area, leading to greater sensitivity (Chapman, 1982), a quality necessary for trace detection of odorant molecules; and c) the fact that a larger outline area should increase the chance of molecule capture (Kaissling, 1971). The third reason we chose to study molecule capture in *Rhipicera* beetles is that their antennal surface is rigid, a property likely to facilitate future simulations of molecule capture, and perhaps lend itself to replication in an artificial sensor.

The particular species we have chosen to study are *Rhipicera carinata* and *Rhipicera femorata*, inhabitants of Western and Eastern Australia, respectively (Hawkeswood, 2000; Jin et al., 2013). We chose *R. carinata* because one of us (TFH) was able to make some behavioural observations of this species in the field. We chose *R. femorata* because we had access to a good quality preserved male specimen of this species, in which both antennae were fanned and intact (Fig. 1). Although we had access to preserved male specimens of the other four *Rhipicera* species, they were not of such good quality. For these reasons, we limited ourselves to just two of the five currently recognised species in the genus *Rhipicera*.

Based on the sexual dimorphism of the antennae of *Rhipicera*, we hypothesised that an important function of the antennae of male *Rhipicera* beetles is to detect the scent associated with female conspecifics. Given this hypothesis, our objective was to investigate the factors that may influence molecule capture by the antennae of male *Rhipicera* beetles - the behaviour of the beetles, and the gross morphology,

4

morphometry, and ultrastructure of their antennae - so that we might use the results in a future simulation of the capture process. Morphometric data in particular are critical to understanding the sensory performance of an antenna (Zacharuk, 1985). In attempting to meet this objective, we have collected some evidence consistent with the notion that male *Rhipicera* beetles locate female conspecifics by olfaction. In addition, we wished to compare our results with similar ones for two species of male moth, namely *B. mori* and the saturniid moth *Antheraea polyphemus*, because the large, elaborate, pectinate antennae of these moths are considered to be an adaptation to maximise molecule capture (Steinbrecht, 1984). Furthermore, the antennae of these moths are a well-documented system for capturing molecules (Schneider and Kaissling, 1956, 1957; Boeckh et al., 1960; Kaissling and Priesner, 1970; Steinbrecht, 1970, 1973, 1987; Kochansky et al., 1975; Vogel, 1983; Kanaujia and Kaissling, 1985; Loudon and Koehl, 2000; Loudon and Davis, 2005). Thus, the antennae of these moths may be used as a standard to gauge how well other relatively large, elaborate antennae capture molecules. To make the comparison with the two moths, we have obtained some morphometric data on the antennae of *A. polyphemus* that was missing from the scientific literature.

MATERIALS AND METHODS

Behaviour of *Rhipicera carinata*

The behaviour of adult *Rhipicera carinata* beetles was observed in the garden of a domestic residence in Spearwood, Perth, Western Australia on 3 and 25 April 2014 (early afternoon and morning, respectively). The garden contained a large mulberry tree (*Morus* sp.), an olive tree (*Olea europaea*), and a bamboo thicket. There was a light variable breeze during both visits; towards the end of the first visit the breeze became stronger, and was directed from the west/south west. The temperature on both visits was 24 – 26 °C.

Specimens

The specimens we used belong to the collections of the Natural History Museum, London. Their catalogue numbers (preceded by 'BMNH[E]') are: 1269005 (male *Rhipicera femorata,* Fig. 1); 1269006 (female *R. femorata*, Fig. 1A); 1269355 (male *R. carinata*), and 1269356 (female *R. carinata*). The male specimen of *Antheraea polyphemus* does not have a catalogue number.

Antennal Nomenclature and Descriptions of Sensilla

In insects, there are three antennal regions (Crowson, 1981; Gullan and Cranston, 2000). These regions are (proximal to distal) the scape, the pedicel, and the flagellum (Nichols, 1989). The scape and pedicel comprise one segment each; the flagellum comprises a variable number of segments. For descriptions of the types of sensilla encountered in this report see Schneider (1964), Kaissling (1971, Fig. 5), and Meinecke (1975).

X-Ray Microcomputed Tomography

X-ray microcomputed tomography (micro-CT) of the heads of the male and female specimens of *R. femorata*, and the head of the male specimen of *A. polyphemus*, was performed at Nikon Metrology, Tring, UK, using an XT H 225 ST system. We removed the wings of the specimen of *A. polyphemus* prior to the scan to place it as close as possible to the X-ray source, thereby maximising the resolution of the scan. X-rays were generated from the target that was fitted to the X-ray micro-CT system at the time: a rotating tungsten reflection target (male *R. femorata*) or static molybdenum

6

reflection target (*A. polyphemus* and female *R. femorata*). The accelerating voltage and current were 55 kV and 543 μA (male *R. femorata*), 45 kV and 446 μA (female *R. femorata*), and 70 kV and 166 μA (*A. polyphemus*). The accelerating voltage for each X-ray scan was determined by the size and density of the sample; the current was chosen such that the signal-to-noise ratio, scan time, and image resolution were optimal. A total of 3,142 projections were collected for each specimen in a single 360° rotation at 0.11458° intervals. The projections were transformed into a three-dimensional matrix using CT-Pro (Version 4.1, Nikon Metrology). The voxel size of each scan was 9.3 μm x 9.3 μm x 9.3 μm (male *R. femorata*), 6.1 μm x 6.1 μm x 6.1 μm (female *R. femorata*), and 13.6 μm x 13.6 μm x 13.6 μm (*A. polyphemus*). For anatomical reconstruction, each scan was converted into a set of TIFF images using the software VGStudio MAX (Version 2.2, Volume Graphics GmbH, Heidelberg, Germany). In the X-ray micro-CT scan of the male specimen of *R. femorata*, both antennae are intact, but in that of the female specimen of *R. femorata*, whilst the right antenna is intact, the left antenna comprises flagellar segments F1-F6 only.

Anatomical Reconstruction

The heads of the specimens of *R. femorata* and *A. polyphemus* were reconstructed using the image processing software ScanIP (Versions 5 to 7, Simpleware, Exeter, UK) as follows. The set of TIFF images from an X-ray micro-CT scan were imported into ScanIP and segmented using the Threshold tool, creating a 'mask' of the head (Howard et al., 2013). Masks of individual antennae were isolated from the head using the Crop and 3D editing tools by severing the joint between the pedicel and the first flagellar segment (*R. femorata*, Fig. 2A and F) or cutting on the proximal edge of the most proximal flagellar segment (*A. polyphemus*; it was difficult to detect the two pedicels in this mask). A morphological filter ('Close') was then applied, using an isometric structuring element (ball) with a radius of 1 or 2 pixels in the *x*, *y* and *z* directions. The part of the antennal mask corresponding to a claw on the right foreleg caught in the right antenna of the male specimen of *R. femorata* (Fig. 1B, box I) was detached using the 3D editing, Floodfill and Paint tools. Masks of individual antennae were filled using the Floodfill tool. Masks of individual flagellar segments were obtained by using the 3D editing tool to remove antennal sections proximal and distal to their bases. Models of antennae and flagellar segments were generated from the

appropriate masks with 10 iterations of triangle smoothing, no reduction of triangles on the surface of the models, and with the 'use greyscale values' button in ScanIP's Model configuration dialogue box activated, to ensure inclusion of information from 'partial volume' voxels (pixels at the antenna/air interface not wholly representative of either), thereby leading to a smoother and more accurate model (Young et al., 2008). Models were exported as binary stereolithography (STL) files.

Morphometric Analysis

Antennal dimensions (Fig. 2) - height (H), width (W), length parallel to presumed direction of airflow (L), and outline area (OA) - were obtained by importing into Rhinoceros (Robert McNeel and Associates, Version 4) the STL file of the appropriate model and proceeding according to the methodology of Cox (2008) and Howard et al. (2013). The number of significant figures given in Table 1 takes into account the error in these measurements. Dimensions of the flagellar segments of *R. femorata* (Fig. 2) - length (*Le*), width at widest point (*w*), thickness at widest point (*T*) - and the depths (*De*) of antennal channels (AC; an antennal channel is the space between two neighbouring flagellar segments: Fig. 2A, B, E and F) - were obtained using the Measurement line tool in ScanIP. Depths of antennal channels were measured between the tips of two adjacent flagellar segments (Fig. 2E) or, in the case of the antennal channels formed by flagellar segments F1-F6 of the male specimen of *R. femorata*, between the tip of the first flagellar segment and the closest point on the proximal surface of the opposing flagellar segment. We obtained dimensions of: all flagellar segments and antennal channels of both antennae of the male specimen of *R. femorata*; all flagellar segments of the right antenna of the female specimen of *R. femorata*, but only the depths of its first seven channels (flagellar segments F8-F21 were partially or completely fused); and the first six flagellar segments of the left antenna of this specimen (the antenna was broken; Fig. 1A). The errors in these dimensions are: ± 0.015 mm (length); ± 5 μm (width); ± 5 μm (thickness); and ± 10 μm (depth of antennal channel).

Surface areas of antennal models and individual flagellar segments were calculated in ScanIP using the Model Statistics tool. The contribution of the area of the 'cut' surface (asterisk, Fig. 2C and G) of flagellar segment F1 to the total surface area of

the antennal models of *R. femorata* was negligible (≤ 0.3 %). The total surface area of each antenna of the specimen of *A. polyphemus* was estimated by adding the surface area of each antennal model (176-197 mm^2) to the product of the number of pheromone-receptive sensilla trichodea (55,000; Boeckh et al., 1960, Table 2) and the surface area of one of these sensilla (0.0026 - 0.0032 mm^2; Keil, 1984, Table 1). Although we verified using a stereomicroscope the presence of the pheromone-receptive sensilla trichodea on the antennae of the specimen of *A. polyphemus*, these sensilla were not resolved in the X-ray micro-CT scan of this specimen. The error in the total surface area of each single antenna is ± 1 mm^2 (male and female *R. femorata*) and ± 25 mm^2 (*A. polyphemus*). These errors take into account: a) the uncertainty in the thresholding procedure used to generate the antennal masks (all three specimens); b) the total surface areas of the models of both of the insect's antennae (male specimen of *R. femorata*, and *A. polyphemus*); and c) the partially or completely fused flagellar segments (F8-F21) of the right antenna of the female specimen of *R. femorata*. We obtained the surface area of only the first six flagellar segments of the left antenna of the female specimen of *R. femorata* (because the antenna was broken), and of only the first seven flagellar segments of the right antenna of this specimen (because flagellar segments F8-F21 were partially or completely fused). The surface areas of the flagellar segments are corrected for the presence of their cut surface(s). The error in the surface area of each flagellar segment is ± 0.05 mm^2.

Reynolds Numbers and Diffusion Times

Reynolds numbers (*Re*) for a) each whole antenna of the male specimen of *R. femorata* and b) this specimen's antennal channels were calculated using the equation (Chance and Craig, 1986; Vogel 1994):

$$Re = \frac{UL}{v}$$

where in this case *U,* the speed of the fluid, is 1 - 7 m/s (the air speeds likely to be encountered by male *Rhipicera* beetles, based on a consideration of Hawkeswood [2000], Conway et al. [2006, Table 2.1] and Nachtigall and Hanauer-Thieser [1992]), *L,* the characteristic linear dimension of the object, is 2 - 3 mm (the length of the antenna parallel to the flow; Table 1) or 100 - 490 µm (lower and upper limits of the

depth of the antennal channels, respectively; Table 1), and ν, the kinematic viscosity of air at 25 °C, is 1.6 x 10^{-5} m^2 s^{-1} (calculated from Denny, 1993, Figs. 4.1 and 5.2). The time (t) taken to diffuse from the centre of the antennal channel of the male specimen of *R. femorata* was calculated using the equation (Berg, 1983):

$$t = x^2/2D$$

where in this case x, the distance diffused, is 50 - 245 μm (half the lower and upper limits of the depth of the antennal channels, respectively; Table 1), and D, the diffusion coefficient of the species diffusing, is taken to be that for bombykol, the female sex pheromone of *Bombyx mori*, i.e. 2.5 x 10^{-6} m^2 s^{-1} (Adam and Delbrück, 1968). Reynolds numbers and diffusion times are given to one significant figure.

Ultrastructure of the Antennae of *R. femorata* and *R. carinata*

Scanning electron microscopy (SEM) of the antennae of the male and female specimens of *R. femorata* and *R. carinata* was performed at the Natural History Museum, London, with a Quanta 650 FEG variable pressure scanning electron microscope (FEI, Oregon, USA) operating at 10 kV and a chamber pressure of 70 Pa (air), and using a secondary electron detector. We assumed that the antennal surfaces of these specimens had remained intact post-mortem, and therefore the structures observed in the micrographs had a similar appearance *in vivo*. Due to the fragility of the antennae, we made no attempt to remove extraneous particles (Fig. 1B, box III) from the antennal surfaces prior to SEM. Specimens were mounted on a motorised tilt-and-rotate stage (Deben, UK) fitted to the Quanta 650 FEG's in-built stage, an arrangement that enabled us to obtain micrographs with unobstructed views of many of the faces of the individual flagellar segments of the antennae of the male specimen of *R. femorata*.

Analysis of the sensilla placodea on the antennae of *R. femorata* and *R. carinata* was performed by reading the appropriate micrograph (dimensions 3,072 pixels x 2,048 pixels, or 1,536 pixels x 1,024 pixels) into Rhinoceros and then proceeding according to the methodology of Cox (2008) and Howard et al. (2013). The antennae of the male and female specimens of *R. femorata* were damaged as the specimens were being

mounted during one SEM session (flagellar segments F16-F36 broke from the male's right antenna; flagellar segments F7 onwards broke from the female's left antenna). Consequently, to avoid further damage, we restricted the SEM of both these specimens and those of *R. carinata*. Therefore, the ultrastructural analysis was not exhaustive. We calculated the average distance between the centre of a sensillum placodeum and the centre of each of its nearest neighbours for eight sensilla placodea on the inner face of flagellar segment F16 on the right antenna of the male specimen of *R. femorata*. The eight sensilla placodea were chosen such that a) no distance was counted twice and b) the flat upper surfaces of the sensilla placodea were judged to be perpendicular to the electron beam. The error in the number of sensilla on a particular face of a flagellar segment is ± 10 sensilla. The density of the sensilla placodea on a particular flagellar segment of the male antenna of *R. femorata* was estimated knowing the number of sensilla placodea on one face of that flagellar segment and the surface area of that flagellar segment. The sensilla placodea were assumed to be uniformly dispersed. The error in the lowest and highest density of sensilla placodea (Table 3) is ± 44 sensilla mm^{-2} and ± 30 sensilla mm^{-2}, respectively. The percentage surface area of a flagellar segment on the male antenna of *R. femorata* occupied by the sensilla placodea was calculated: a) knowing the number of sensilla placodea on one face of the flagellar segment; b) knowing the surface area of that flagellar segment; and c) assuming that each sensillum placodeum was circular, with a diameter of 22 μm (the average diameter of a sensillum placodeum on this antenna).

11

RESULTS

Behaviour of *Rhipicera carinata*

Adult male *Rhipicera carinata* beetles were observed perching in prominent positions on high points in the garden at Spearwood, including the tips of bamboo stems, the top of both a mulberry tree and a wire fence, and the tops of both wooden posts and metal poles (Fig. 3A). These positions were usually occupied by a single individual, with the beetle generally still, upright, and facing into the breeze (Fig. 3A). Male beetles observed in flight swept laterally across distances of 1 or 2 m, and approached the mulberry tree and an olive tree, and other high points from the leeward side, re-orientating themselves to fly into the wind if the wind changed direction, sometimes hanging almost stationary. The antennae of male beetles were fanned when perching or flying (Fig. 3; Video 1). We refer to the fanned form of the antenna as its alert state (Fig. 4A). Adult female *R. carinata* beetles were also found on high points (e.g. dead branches in the olive tree, posts, and a wire fence). Flying and crawling male beetles took some time to locate female beetles in these positions. Male beetles could fold their antennae into a banner-like form when copulating with female beetles. We refer to the banner-like form of the antenna as its relaxed state (Fig. 4B). We did not observe any behaviour which suggested that female beetles produce sound to attract male beetles.

Gross Morphology of the Antennae of *Rhipicera femorata*

Male antennae. The antennae of male *Rhipicera* beetles (Jin et al., 2013, Fig. 3) are lamellate (Nichols, 1989). In the male specimen of *Rhipicera femorata* that we studied, the antennae are fanned, corresponding to the alert state observed *in vivo* (see previous section and Fig. 4A), with a ventral gap in the fan (Gp, Figs. 1B and 2A; Video 2). The concave region of the fan faces anteriorly (Fig. 2B). Each antenna in this specimen comprises 38 segments, consistent with the 32-40 segments expected for the antennae of male *R. femorata* beetles (Jin et al., 2013). The 38 antennal segments include (proximal to distal): the scape (Sc), the pedicel (Pe), and 36 flagellar segments (F1-F36; Fig. 2A). The scape and pedicel, together with the first few flagellar segments, ensure that the majority of the antenna is held away from the body (Figs. 1B and 2A). Inspection of the dorsal view of the specimen's head suggests that

the right antenna has been bent back slightly, possibly as a result of it becoming entangled with a claw on the right foreleg (Fig. 1A, small arrow, and Fig. 1B, box I).

The morphology of the flagellar segments varies across the antenna (Fig. 2A). Thus, segment F1 is short and broad, whereas segments F2-F36 are more elongated. Segments F2-F5 are relatively straight, whereas segments F6-F36 have a broad, curved, blade-like region (Fig. 2C, Bl) whose concave face is directed towards the distal part of the antenna (Fig. 2D).

Female antennae. The antennae of female *Rhipicera* beetles differ in morphology from those of male *Rhipicera* beetles (Jin et al., 2013, Fig. 3). Thus, the antennae of female *Rhipicera* beetles may be described as serrate rather than lamellate (Nichols, 1989), and they are not fanned. In the specimen we studied, the right antenna comprises 23 segments (Fig. 2F), consistent with the 22-28 segments expected for the antennae of female *R. femorata* beetles (Jin et al., 2013), but less than the number of segments in the male antennae. The 23 antennal segments include (proximal to distal): the scape, the pedicel, and 21 flagellar segments (F1-F21; Fig. 2F). The flagellar segments are shorter than they are in the male (Fig. 5A and Table 1), and all are straight. The left antenna is broken, and comprises only flagellar segments F1-F6.

Morphometry and Physical Characteristics of the Antennae of *R. femorata*
The morphometry and physical characteristics of the antennae of *R. femorata* are shown in Fig. 5, and Tables 1 and 2.

Ultrastructure of the Antennae of *R. femorata* and *R. carinata*
On inspection of the micrographs of the antennal surface of both the male and female specimens of *R. femorata*, it was immediately apparent that there were many sensilla placodea on the male antennae, but very few on the female antennae. Given this marked sexual dimorphism, we focus here on the sensilla placodea, although we note that sensilla basiconica and sensilla trichodea are also present on the male antennal surface (Fig. 6C, D and F).

The sensilla placodea on the antennae of the male specimen of *R. femorata* are flat, disk-like structures (average diameter 22 μm, n = 22 sensilla) that protrude slightly

(by 3 - 4 µm, n = 12 sensilla) from the antennal surface (Fig. 6C, large highlighted region)[2]. The intense spots of reflected light seen on the antennal surface when the antennae are photographed using a flash light, or when the antennae are viewed under the stereomicroscope with a light source, are presumably caused by the flat upper surface of each sensillum placodeum acting as a mirror (Fig. 1B, box II).

The sensilla placodea of the male specimen of *R. femorata* are present on all the flagellar segments, but are absent from the dorsal surfaces of the scape and pedicel (we did not investigate the ventral surfaces of the scape and pedicel). Consequently, we excluded the scape and pedicel when we calculated the surface area of the whole antenna. The sensilla placodea are well dispersed over the stem of each flagellar segment (Fig. 6C; the stem of the flagellar segment is defined in Fig. 2C), with an average distance of 39 µm (n = 51) between the centres of neighbouring sensilla placodea. The sensilla placodea are present on the anterior and ventral parts of the base of each flagellar segment (Fig. 6F), but are virtually absent from the posterior part of the base of each flagellar segment (Fig. 6G; the base of the flagellar segment is defined in Fig. 2C). The majority of the sensilla placodea are found on the stem of each flagellar segment (96 - 99 %, n = 16 flagellar segments).

We found that the number of sensilla placodea on a given face (inner or outer) of a given flagellar segment is about the same on each antenna of the male specimen of *R. femorata* (Table 3, entries for F15, F25, F26, F28, F29 and F31-F36), suggesting that a) the distribution of sensilla placodea on both antennae is symmetrical, and b) the total number of sensilla placodea on each antenna is about the same. The density of the sensilla placodea on the flagellar segments, where we were able to estimate it, varies from 171 ± 44 mm^{-2} to 665 ± 30 mm^{-2}, with the density lowest at the extremities of each antenna (Table 3). The average density of the sensilla placodea is 560 mm^{-2}. Using these figures for density, together with the total surface area of each antenna (52-54 mm^2, Table 1), the total number of sensilla placodea on each antenna is likely to fall in the range 6,000 – 38,000 (this range takes into account the error in both the measurement of the densities and the total surface area of the antenna), and might be expected, from the average density, to be close to 30,000 (Table 4). The percentage surface area of each flagellar segment occupied by the sensilla placodea

varies from 6 – 26 % (n = 31 flagellar segments). The average percentage surface area of each flagellar segment occupied by the sensilla placodea is 21 %, a relatively low figure that reflects the fact that the sensilla basiconica are interspersed between the sensilla placodea, i.e. another type of receptor is present on the antennal surface (Fig. 6D).

The sensilla placodea on the left antenna of the female specimen of *R. femorata* are similar in appearance to those on the male antennae, although the female sensilla placodea appear to have a smaller average diameter (15 μm, n = 19 sensilla). We counted a total of just 27 sensilla placodea on the dorsal surface of the left antenna of the female specimen before it broke. These sensilla were scattered across flagellar segments F7-F21, with 0 – 5 sensilla placodea per flagellar segment. Assuming that the number of sensilla placodea is similar on both antennal surfaces, we estimate that the number of sensilla placodea on each female antenna will be no more than 100.

The ultrastructure of the antennal surfaces of the male and female specimens of *R. carinata* is similar to that of their *R. femorata* counterparts (males: compare Fig. 6C and D with Fig. 7A and C; females: compare Fig. 6B and E with Fig. 7B and D). Thus, there appear to be many more sensilla placodea on the male antenna of *R. carinata* than on the conspecific female antenna (compare Fig. 7A and D). In addition, the average diameter of the sensilla placodea on the antenna of the male specimen of *R. carinata* is 20 μm (n = 22) and on the antenna of the female specimen of *R. carinata* is 11 μm (n = 5), similar to the average diameters of the sensilla placodea on the antennae of the male and female specimens of *R. femorata* (22 and 15 μm, respectively).

DISCUSSION

Evidence Consistent with the Notion that Male *Rhipicera* Beetles Locate Female Conspecifics by Olfaction

Three pieces of evidence are consistent with the notion that male *Rhipicera femorata* and *Rhipicera carinata* beetles locate female conspecifics by olfaction:

1) Behaviour in the field of *R. carinata*. The wavering flight of male *R. carinata* beetles is reminiscent of the zigzagging behaviour of scent-tracking animals, including insects (Kennedy, 1986; Roper, 1999; Porter et al., 2007). Male beetles fly upwind, or face the wind when perching, behaviour that is also typical of a scent-tracking animal (e.g. Cardé and Charlton, 1984, Table 1; Roper, 1999). That it took some time for male beetles to locate the female beetles when they were close to the latter suggests that sight does not play a major part in the location process, at least in the final stage. Nor does hearing seem to play a part, because we did not observe female beetles making any sounds to attract male beetles (e.g. tapping the substrate). Furthermore, *Rhipicera* beetles do not have a stridulatory apparatus with which to make sound (Wessel, 2006, Table 30.1).

2) Elaborate antennal architecture of male *R. femorata* and *R. carinata*. There are several well documented cases of antennal sexual dimorphism in insects where it is known that the more elaborate male antenna is an adaptation for locating female conspecifics at a distance by olfaction ('at a distance' implies that the male antenna is able to detect trace quantities of odorant molecules). These cases comprise saturniid moths (Lepidoptera, Saturniidae; Rau and Rau, 1929; Boeckh et al., 1960; Kochansky et al., 1975), diprionid sawflies (Hymenoptera, Diprionidae; Coppel et al., 1960; Jewett et al., 1976; Hallberg, 1979; Hansson et al., 1991; Anderbrant et al., 1995; Krogmann et al., 2013), and melolonthine beetles (Coleoptera, Scarabaeidae; Meinecke, 1975; Ruther et al., 2000, 2002a,b; Reinecke et al., 2002a,b, 2005, 2006). Field tests with the Western banded glowworm, *Zarhipis integripennis* (Coleoptera, Phengodidae) also indicate that adult male beetles, which have distinct pectinate antennae, locate adult (larviform) female conspecifics by scent (Tiemann, 1967). A note of caution should be struck here, however: antennal sexual dimorphism is not always associated with the trace detection of odorant molecules. The plumose

16

antennae of male mosquitos are, for example, adaptations for acoustic communication (Göpfert et al., 1999).

3) Ultrastructure of the antennae of *R. femorata* and *R. carinata*. The antennae of male *R. femorata* beetles possess numerous sensilla placodea (an estimated 30,000 per antenna; Table 4), but there are very few sensilla placodea on the female's antennae (an estimated 100 per antenna). There is a similar bias in *R. carinata*. Sensilla placodea in general are considered to be olfactory receptors (Altner, 1977, Table 2), and indeed electrophysiological experiments have shown them to have an olfactory function in beetles (Leal and Mochizuki, 1993, Fig. 2; Renou et al., 1998; Hansson et al., 1999; Bengtsson et al., 2011), bees (Lacher and Schneider, 1963; Lacher, 1964; Kaissling and Renner, 1968; Vareschi, 1971; Akers and Getz, 1992, 1993), a wasp (Hymenoptera, Braconidae; Ochieng et al., 2000), and aphids (Bromley and Anderson, 1982; Dawson et al., 1987, 1990 [Fig. 4]). Most importantly, sensilla placodea have been shown to respond to scent associated with female conspecifics (Kaissling and Renner, 1968; Dawson et al., 1987, 1990 [Fig. 4]; Leal and Mochizuki, 1993, Fig. 2; Hansson et al., 1999). The antennae of the male *Melolontha melolontha* beetle, on which there is a large population of sensilla placodea (Meinecke, 1975, Figs. 2a and 25), have also been shown to respond to scent associated with female conspecifics (Reinecke et al., 2002a,b, 2005).

Sexual dimorphism in the abundance of antennal sensilla, where the male antenna has many more of a particular type of sensillum than the conspecific female antenna, is common in insects in which female sex pheromone is known to be detected by male conspecifics at a distance (Chapman, 1982, Fig. 10), e.g. moths (Boeckh et al., 1960, Table 2; Sanes and Hildebrand, 1976), cockroaches (Blattidae; Blattodea; Schaller, 1978), sawflies (Hallberg, 1979), and beetles (Meinecke, 1975, Fig. 2a and b; Kim and Leal, 2000). Often in such cases, the male has 10,000 more sensilla per antenna than the female (Chapman, 1982). The number of sensilla placodea on the antennae of the drones and workers of honey bees, *Apis mellifera*, exhibit a similar dimorphism (Esslen and Kaissling, 1976). In the two specimens of *R. femorata* that we examined, the male had an estimated 30,000 sensilla placodea per antenna whilst the female had an estimated 100 sensilla placodea on its right antenna. Thus, it appears that the male antenna of *R. femorata* does indeed have at least 10,000 more sensilla placodea than

the female antenna. Note that sexual dimorphism in the number of antennal sensilla is absent in insects that do not seek out mates (Chapman, 1982; Allsopp, 1990; McQuillan and Semmens, 1990; Renou et al., 1998).

Factors Likely to Influence Molecule Capture in Male *Rhipicera* Beetles

Working on the assumption that the antennae of male *Rhipicera* beetles detect scent associated with female conspecifics, we now highlight several factors likely to influence molecule capture by these antennae. Because the morphology and ultrastructure of the antennae of male *R. carinata* and *R. femorata* beetles are similar (to see the similarity in morphology compare Fig. 3D and 3F of Jin et al. [2013]), we believe that the behavioural observations of *R. carinata* are relevant to molecule capture by the antennae of male *R. femorata* and, conversely, that the morphometric analysis of the antennae of *R. femorata* is relevant to molecule capture by the antennae of male *R. carinata*. Consequently, in this section, we do not differentiate between these two species.

The chances of capturing odorant molecules are likely to be improved by four gross morphometric features of the male beetle's antenna, namely its height, width, outline area, and total surface area (Table 1). The relatively large total surface area of the male beetle's antenna will, for example, favour diffusion of molecules to the antennal surface, because the flux of molecules to a surface is proportional to the area of that surface (LaBarbera and Vogel, 1982; Schmidt-Nielsen, 1997).

The chances of capturing odorant molecules will also be improved by the relatively large number of sensilla placodea on the antennae of male *Rhipicera* beetles (Chapman, 1982; Steinbrecht, 1984), together with the location and dispersal of these sensilla on the antennal surface. Thus, the sensilla placodea are located where transport of odorant molecules to the antennal surface is most likely to occur when air bearing odorant molecules impinges on the antenna, namely on the stem of each flagellar segment, and on the anterior section of the base of each flagellar segment (Fig. 6C and F; see Fig. 2C for the definition of the base and stem of a flagellar segment). There are, however, very few sensilla placodea on the posterior section of the base of each flagellar segment, presumably because flow does not impinge on this region (Fig. 6G). The pheromone-receptive sensilla of the male hawkmoth *Manduca*

sexta (Lepidoptera, Sphingidae) are similarly orientated windward (Keil, 1989). Most odorant molecules are likely to be captured on the stems of the flagellar segments, where the majority (96 – 99 %) of the sensilla placodea are found (Fig. 6C). In addition, the sensilla placodea are well dispersed (the average distance between the sensilla placodea is 39 μm), as expected for a surface that captures molecules efficiently (Berg and Purcell, 1977; Berg, 1983). Furthermore, because the sensilla placodea cover only a small percentage (6 – 26 %) of the surface of the flagellar segment, other receptor systems (here the sensilla basiconica) can be interspersed between the sensilla placodea (Fig. 6C, large highlighted region, and Fig. 6D), potentially allowing the antenna to perform simultaneously different chemosensory functions (Berg and Purcell, 1977; Berg, 1983).

Reynolds numbers for the whole antennae fall in the range 100 – 1,000 (Table 2). At the lower end of this range, flow is laminar, but at the higher end flow may be making the transition from laminar to turbulent (Chance and Craig, 1986). Both types of flow will affect transport of odorant molecules to the antenna. Note also that, over this entire range of Reynolds numbers, vortices are likely to be shed from each antenna (Vogel, 1994, Fig. 5.5c).

Boundary layers – regions of slower moving fluid formed when bulk fluid passes over a solid surface (Sutton, 1949; Denny, 1993) – may limit transport of odorant molecules to a sensory surface (Vogel, 1994). Several behavioural and anatomical factors may be acting to reduce the effect of the various boundary layers that may be associated with male *Rhipicera* beetles. First, ground-based male *Rhipicera* beetles adopt prominent positions on the object on which they are perched (e.g. a wire fence), suggesting an attempt to avoid the local boundary layer of that object (Fig. 3A). Second, the scape and pedicel, together with the first few flagellar segments, ensure that the antenna of the male beetle protrudes laterally (Fig. 2A), away from the boundary layer that will be associated with the body. Third, the sensory surface of the male beetle's antenna, rather than being one large, complete surface over which a relatively thick boundary layer would develop, is partitioned into many smaller surfaces. For the same reason, the uptake of carbon dioxide by plants is likely to be more effective with many small leaves than with a few large ones (Denny, 1993).

The stems of the flagellar segments may be regarded as a series of parallel plates, and the gaps between the flagellar segments thin rectangular channels (Vogel, 1994, Fig. 13.4). Flow through each antennal channel (AC, Fig. 2A, B and E) will be driven by a pressure difference generated either by the beetle moving, or by an external current of air, or both. The relatively short width of the flagellar segments (Fig. 5B and Table 1) will reduce the cost of moving fluid through the antennal channels (LaBarbera and Vogel, 1982). At the air speeds likely to be encountered by the male beetles when flying or perching, flow in the antennal channels will be laminar (Reynolds numbers falling in the range 10 – 200; Table 2). According to Martinelli and Viktorov (2009, equation 6), at the lower end of this range the velocity profile of flow in an antennal channel is likely to develop from flat to parabolic (Levich, 1962, Fig. 20; Vogel, 1994, Figs. 13.3 and 13.4). Where the velocity profile is flat, the flux of odorant molecules to the antennal surface will be a function of the distance from the upstream edge of the flagellar segment (Levich, 1962, Fig. 18). Where the velocity profile is parabolic, however, the flux of odorant molecules to the antennal surface is likely to be a function of both the distance from the upstream edge of the flagellar segment and the depth of the antennal channel (Levich, 1962). Also according to Martinelli and Viktorov (2009, equation 6), at the upper end of the range of Reynolds numbers for flow in the antennal channels, the velocity profile in each channel is likely to remain flat, and therefore the flux of odorant molecules to the antennal surface will be a function solely of the distance from the upstream edge of the flagellar segment (Levich, 1962). The time taken for odorant molecules to diffuse from the centre of each thin channel to the antennal surface is likely to be short (0.5 – 10 ms; Table 2).

Flow of air through the antennal channels of the male beetle will be facilitated by: a) the male beetle perching on high points, where it may exploit the higher wind speeds associated with the more distal region of a boundary layer (here created by the air moving over the ground; Vogel 1994); b) the upright stance of the male beetle when perching or flying – such a stance should minimise downwind obstructions (Fig. 3A; Video 1); c) the antennae protruding from the body (Figs. 1B and 2A); and d) the relatively thin flagellar segments, which are likely to make the antennae 'leaky' (Koehl, 1995, Fig. 3; compare the thickness of the male flagellar segments with the thickness of the female flagellar segments, and with the depth of the male antennal

20

channels, in Fig. 5C and D, and Table 1). In other words, a significant proportion of the air impinging on the antenna is likely to pass through it, rather than around it, aiding molecule capture.

Comparison with the Scent-Capturing Ability of a Pectinate Antenna

Although a true comparison of the molecule-capturing ability of the lamellate antenna of a male *Rhipicera* beetle with that of the pectinate antenna of the male silk moth *Bombyx mori* and the male saturniid moth *Antheraea polyphemus* - a well-documented system considered to be an adaptation to maximise molecule capture (Steinbrecht, 1984) - must await flow simulations (see below), we can at least make some inferences from a comparison of the morphometry and ultrastructure of the two types of antenna (Tables 1 and 4). Thus, the height, width, outline area, and total surface area of the antenna of *A. polyphemus* are all greater than the same measurements for the specimen of the male *R. femorata* beetle examined in this study, as is the total number of pheromone-receptive sensilla trichodea. On the other hand, the outline area of the antenna of the specimen of the male *R. femorata* beetle, together with the estimated total number of sensilla placodea, are greater than the equivalent figures for *B. mori*. But the total surface area of the antenna of *B. mori* is greater than the total surface area of the antenna of the male *R. femorata* beetle. Based on this comparison, we might conclude that the molecule-capturing ability of the antenna of the male *R. femorata* beetle is similar to that of the antenna of the male silk moth *B. mori*, but is not as good as that of the antenna of the male saturniid moth *A. polyphemus*. We note, however, that this comparison does not take into account the number of odorant receptor cells in each sensillum, because we do not yet know this number for male *R. femorata* beetles. We note also that the physical structures for molecule capture are different in the three insects. Thus, the putative odorant-receptive sensilla placodea of the male *R. femorata* beetle are located on a series of thin parallel plates whereas the pheromone-receptive sensilla trichodea of the male *A. polyphemus* and male *B. mori* moths are located on branches arising from the antennal stem (Boeckh et al., 1960, Fig. 3; Steinbrecht, 1973, Fig. 1). Furthermore, the sensilla placodea of the male *R. femorata* beetle are plate-like, whereas the sensilla trichodea of the male *A. polyphemus* and male *B. mori* moths are hair-like. These structural differences are likely to have a significant bearing on molecule capture (Steinbrecht, 1987).

Future Work

In the future, we hope to simulate flow in the antennal region of male *R. femorata* beetles using a model of the antenna as described here, and artificial variations of this model. We will then use the flow simulations to determine how efficient the model antenna is at capturing odorant molecules. In performing the flow simulations, we hope to determine whether the antenna has any mechanisms for reducing drag (such mechanisms may in turn reduce the possibility of damage to the antenna, and reduce the cost of flying). We note that living structures whose concave sides are directed into the flow, as the antennae of *Rhipicera* are thought to be (Figs. 2B and 3A), have high drag coefficients (Vogel, 1994, Fig. 6.5). We also hope to determine how the curvature of the flagellar segments influences flow.

Finally, it will be vital to acquire further evidence to support the hypothesis that an important function of the antennae of male *Rhipicera* beetles is to detect the scent associated with female conspecifics. One could acquire this evidence by following well established procedures in chemical ecology (e.g. Zhang et al., 2003; Molnár et al., 2009). Thus, in outline, one would first need to determine, using traps baited with single virgin females (together with unbaited control traps), whether male *Rhipicera* beetles fly to female conspecifics. If males were shown conclusively to fly to virgin females, one would then attempt to isolate and characterise the chemical(s) attracting males to females, e.g. by passing the air from a glass vessel containing virgin females through an adsorbent material (e.g. charcoal), eluting any chemical(s) bound to the adsorbent material with a suitable organic solvent, and then analysing the resultant extract by gas chromatography with simultaneous electroantennographic detection. In this procedure, the extract, in gaseous form, would be passed over an antennal preparation. From the resultant electroantennogram one may be able to deduce, by comparison with the appropriate chemical databases, the biologically active components of the extract (providing they are known compounds). One could then use synthetic versions of these components in laboratory bioassays and field tests to determine whether the synthetic versions attract female *Rhipicera* beetles. One might also consider electrophysiological experiments on single sensilla placodea on the male antenna to identify the biologically active components in the female extract these sensilla respond to (see, for example, Leal and Mochizuki, 1993). In addition,

transmission electron microscopy could be used to characterise the cellular composition of the sensilla placodea (Zacharuk, 1985; Steinbrecht, 1996), and, in particular, to inspect the walls of the sensilla placodea for pores. Multiple 'wall pores' are a characteristic feature of odorant-receptive sensilla (Altner, 1977; Altner and Prillinger, 1980, Table 1; Steinbrecht, 1984, 1987 [Fig. 8], 1996; Zacharuk, 1985).

LITERATURE CITED

Adam G, Delbrück M. 1968. Reduction of dimensionality in biological diffusion processes. In: Rich A, Davidson N. Structural chemistry and molecular biology. San Francisco: London. p 198-215.

Ågren L. 1985. Architecture of a lamellicorn flagellum (*Phyllopertha horticola*, Scarabaeidae, Coleoptera, Insecta). J Morph 186: 85-94.

Akers RP, Getz WM. 1992. A test of identified response classes among olfactory receptor neurons in the honey-bee worker. Chem Senses 17: 191-209.

Akers RP, Getz WM. 1993. Response of olfactory receptor neurons in honeybees to odorants and their binary mixtures. J Comp Physiol A 173: 169-185.

Allsopp PG. 1990. Sexual dimorphism in the adult antennae of *Antitrogus parvulus* Britton and *Lepidiota negatoria* Blackburn (Coleoptera: Scarabaeidae: Melolonthinae). J Aust Ent Soc. 29: 261-266.

Altner H. 1977. Insect sensillum specificity and structure: an approach to a new typology. In: LeMagnen J, MacLeod P, editors. Olfaction and taste VI. London: Information Retrieval. p 295-303.

Altner H, Prillinger L. 1980. Ultrastructure of invertebrate chemo-, thermo-, and hygroreceptors and its functional significance. Int Rev Cyt 67: 69-139.

Anderbrant O, Hansson BS, Hallberg E, Geri C, Varama M, Hedenström E, Högberg HE, Fägerhag J, Edlund H, Wassgren AB, Bergström G, Löfqvist J. 1995. Electrophysiological and morphological characteristics of pheromone receptors in male pine sawflies, *Diprion pini* (Hymenoptera: Diprionidae), and behavioural response to some compounds. J Insect Physiol 41: 395-401.

Bengtsson JM, Khbaish H, Reinecke A, Wolde-Hawariat Y, Negash M, Seyoum E, Hansson BS, Hillbur Y, Larsson MC. 2011. Conserved, highly specialized olfactory

receptor neurons for food compounds in 2 congeneric scarab beetles, *Pachnoda interrupta* and *Pachnoda marginata*. Chem Senses 36: 499-513.

Berg HC, Purcell EM. 1977. Physics of chemoreception. Biophys J 20:193-219.

Berg HC. 1983. Random walks in biology. Princeton: Princeton University Press.

Boeckh J, Kaissling KE, Schneider D. 1960. Sensillen und Bau der Antennengeissel von *Telea polyphemus* (Vergleiche mit weiteren Saturniden: *Antheraea*, *Platysamia* und *Philosamia*).(Sensilla and construction of the antennal flagellum of *Telea polyphemus* [comparisons with other saturniid moths: *Antheraea*, *Platysamia* and *Philosamia*])*.* Zool Jahrb Anat Ontog 78: 559-584. In German.

Broeckling CD, Salom SM. 2003. Antennal morphology of two specialist predators of hemlock woolly adelgid, *Adelges tsugae* Annand (Homoptera: Adelgidae). Ann Entomol Soc Am 96: 153-160.

Bromley AK, Dunn JA, Anderson M. 1979. Ultrastructure of the antennal sensilla of aphids. I. Coeloconic and placoid sensilla. Cell Tissue Res 203: 427-442.

Bromley AK, Anderson M. 1982. An electrophysiological study of olfaction in the aphid *Nasonovia ribis-nigri*. Ent Exp Appl 32: 101-110.

Cardé RT, Charlton RE. 1984. Olfactory sexual communication in Lepidoptera: strategy, sensitivity and selectivity. In: Lewis T, editor. Insect communication. London: Academic Press. p 241-265.

Chance MM, Craig DA. 1986. Hydrodynamics and behaviour of Simuliidae larvae (Diptera). Can J Zool 64:1295-1309.

Chapman RF. 1982. Chemoreception: the significance of receptor numbers. Adv Insect Physiol 16: 247-356.

Conway A, Reynolds R, Dise N, Dubbin W, Gagan M. 2006. Environmental science: air and earth. Milton Keynes: The Open University.

Coppel HC, Casida JE, Dauterman WC. 1960. Evidence for a potent sex attractant in the introduced pine sawfly, *Diprion similis* (Hymenoptera: Diprionidae). Ann Entomol Soc Am 53: 510-512.

Cox JPL. 2008. Hydrodynamic aspects of fish olfaction. J Roy Soc Interface 5:575-593.

Crowson RA. 1981. The biology of the Coleoptera. London: Academic Press.

Dawson GW, Griffiths DC, Janes NF, Mudd A, Pickett JA, Wadhams LJ, Woodcock CM. 1987. Identification of an aphid sex pheromone. Nature 325: 614-616.

Dawson GW, Griffiths DC, Merritt LA, Mudd A, Pickett JA, Wadhams LJ, Woodcock CM. 1990. Aphid semiochemicals – a review, and recent advances on the sex pheromone. J Chem Ecol 16: 3019-3030.

Denny MW. 1993. Air and water. Princeton: Princeton University Press.

Esslen J, Kaissling KE. 1976. Zahl und Verteilung antennaler Sensillen bei der Honigbiene (*Apis mellifera* L.). (Number and distribution of the sensilla on the antennal flagellum of the honeybee [*Apis mellifera* L.].) Zoomorph 83: 227-251. In German, with an abstract in English.

Fonta C, Masson C. 1987. Structural and functional studies of the peripheral olfactory nervous system of male and female bumble-bees (*Bombus hypnorum* and *Bombus terrestris*). Chem Senses 12: 53-69.

Göpfert M, Briegel H, Robert D. 1999. Mosquito hearing: sound-induced antennal vibrations in male and female *Aedes aegypti*. J Exp Biol 202: 2727-2738.

Gullan PJ, Cranston PS. 2000. The insects. 2nd ed. Oxford: Blackwell Science.

Hallberg E. 1979. The fine structure of the antennal sensilla of the pine saw fly *Neodiprion sertifer* (Insecta: Hymenoptera). Protoplasma 101: 111-126.

Hansson BS, Van der Pers JNC, Högberg HE, Hedenström E, Anderbrant O, Löfqvist J. 1991. Sex pheromone perception in male pine sawflies, *Neodiprion sertifer* (Hymenoptera; Diprionidae). J Comp Physiol A 168: 533-538.

Hansson BS, Larsson MC, Leal WS. 1999. Green leaf volatile-detecting olfactory receptor neurones display very high sensitivity and specificity in a scarab beetle. Physiol Entomol 24: 121-126.

Hawkeswood TJ. 2000. Some notes on the occurrence of the Australian beetle *Rhipicera femorata* (Kirby) (Coleoptera: Rhipiceridae). Mauritiana 17: 417-419.

Howard LE, Holmes WM, Ferrando S, Maclaine JS, Kelsh RN, Ramsey A, Abel RL, Cox JPL. 2013. Functional nasal morphology of chimaerid fishes. J Morph 274: 987-1009.

Jewett DM, Matsumura F, Coppel HC. 1976. Sex pheromone specificity in the pine sawflies: interchange of acid moieties in an ester. Science 192: 51-53.

Jin Z, Escalona HE, Ślipiński A, Pang H. 2013. Phylogeny and classification of Rhipicerinae (Coleoptera: Rhipiceridae) with a review of the Australian taxa. Annales Zoologici 63: 275-317.

Kaissling KE, Renner M. 1968. Antennale Rezeptoren für queen substance und Sterzelduft bei der Honigbiene. (Antennal receptors for queen substance and scent gland odour in honeybees.) Z vergl Physiol 59: 357-361. In German, with an abstract in English.

Kaissling KE, Priesner E. 1970. Die Riechschwelle des Seidenspinners. (The olfactory threshold of the silk moth.) Naturwissenschaften 57: 23-28. In German.

Kaissling KE. 1971. Insect olfaction. In: Beidler LM, editor. Handbook of sensory physiology IV Chemical senses Pt 1. Berlin: Springer-Verlag. p 351-431.

Kaissling KE. 2009. The sensitivity of the insect nose: the example of *Bombyx mori*. In: Gutiérrez A, Marco S, editors. Biologically inspired signal processing, SCI. Vol 188. Berlin: Springer-Verlag. p 45-52.

Kaissling KE. 2014. Pheromone reception in insects: the example of silk moths. In: Mucignat-Caretta C, editor. Neurobiology of chemical communication. Boca Raton: CRC Press. p 99-146.

Kanaujia S, Kaissling KE. 1985. Interactions of pheromone with moth antennae: adsorption, desorption and transport. J Insect Physiol 31: 71-81.

Keil TA. 1984. Reconstruction and morphometry of silkmoth olfactory hairs: a comparative study of sensilla trichodea on the antennae of male *Antheraea polyphemus* and *Antheraea pernyi* (Insecta, Lepidoptera). Zoomorph 104: 147-156.

Keil TA. 1989. Fine structure of the pheromone-sensitive sensilla on the antenna of the hawkmoth, *Manduca sexta*. Tissue Cell 21: 139-151.

Kennedy JS. 1986. Some current issues in orientation to odour sources. In: Payne TL, Birch MC, Kennedy CEJ, editors. Mechanisms in insect olfaction. Oxford: Clarendon Press. p 11-25.

Kim JY, Leal WS. 2000. Ultrastructure of pheromone-detecting sensillum placodeum of the Japanese beetle, *Popillia japonica* Newmann (Coleoptera: Scarabaeidae). Arthropod Struct Dev 29: 121-128.

Kochansky J, Tette J, Taschenberg EF, Cardé RT, Kaissling KE, Roelofs WL. 1975. Sex pheromone of the moth, *Antheraea polyphemus*. J Insect Physiol 21: 1977-1983.

Koehl MAR. 1995. Fluid flow through hair-bearing appendages: feeding, smelling and swimming at low and intermediate Reynolds numbers. In: Ellington CP, Pedley

TJ, editors. Biological fluid dynamics. Symposia of the Society for Experimental Biology. Symposium XLIX. Cambridge: The Company of Biologists. p 157-182.

Koehl MAR. 2006. The fluid mechanics of arthropod sniffing in turbulent odor plumes. Chem Senses 31: 93-105.

Krogmann L, Engel MS, Bechly G, Nel A. 2013. Lower Cretaceous origin of long-distance mate finding behaviour in Hymenoptera (Insecta). J Syst Palaeontol 11: 83-89.

LaBarbera M, Vogel S. 1982. The design of fluid transport systems in organisms. Am Sci 70:54-60.

Lacher V, Schneider D. 1963. Elektrophysiologischer nachweis der Riechfunktion von Porenplatten (sensilla placodea) auf den Antennen der Drohne und der Arbeitsbiene (*Apis mellifica* [sic] L.) (Electrophysiological evidence of olfactory function of pore plates [sensilla placodea] on the antennae of the drone and worker bee [*Apis mellifera* L.].) Z vergl Physiol 47: 274-278. In German, with an abstract in English.

Lacher V. 1964. Elektrophysiologische Untersuchungen an Einzelnen Rezeptoren für Geruch, Kohlendioxyd, Luftfeuchtigkeit und Temperatur auf den Antennen der Arbeitsbiene und der Drohne (*Apis mellifica* [sic] L.) (Electrophysiological studies of individual receptors for odour, carbon dioxide, humidity and temperature on the antennae of the worker bee and the drone [*Apis mellifera* L.].) Z vergl Physiol 48: 587-623. In German, with an abstract in English.

Lawrence JF, Britton EB. 1994. Australian beetles. Victoria: Melbourne University Press.

Lawrence JF. 2005. Dascilloidea Guérin-Méneville, 1843. In: Kristensen NP, Beutel RG, editors. Handbook of zoology. Volume IV. Arthropoda: Insecta. Part 38. Coleoptera, beetles. Volume 1: Morphology and systematics. Berlin: Walter de Gruyter. p 451-460.

Leal WS, Mochizuki F. 1993. Sex pheromone reception in the scarab beetle *Anomala cuprea*. Naturwissenschaften 80: 278-281.

Levich VG. 1962. Physicochemical hydrodynamics. Englewood Cliffs, NJ: Prentice-Hall.

Loudon C, Koehl MAR. 2000. Sniffing by a silkworm moth: wing fanning enhances air penetration through and pheromone interception by antennae. J Exp Biol 203: 2977-2990.

Loudon C, Davis EC. 2005. Divergence of streamlines approaching a pectinate insect antenna: consequences for chemoreception. J Chem Ecol 31: 1-13.

Lu CK, Wang XQ. 2009. Ultrastructure of olfactory sensilla on the antenna of *Proagopertha lucidula* (Coleoptera: Scarabaeidae). Acta Entomol Sin 52: 39-45.

McQuillan PB, Semmens TD. 1990. Morphology of antenna and mouthparts of adult *Adoryphorus couloni* (Burmeister) (Coleoptera: Scarabaeidae: Dynastinae). J Aust Ent Soc 29: 75-79.

Martinelli M, Viktorov V. 2009. Modelling of laminar flow in the inlet section of rectangular microchannels. J Micromech Microeng 19: article number 025013.

Meinecke CC. 1975. Riechsensillen und Systematik der Lamellicornia (Insecta, Coleoptera). (Olfactory sensilla and systematics of the lamellicornia [Insecta, Coleoptera].) Zoomorph 82: 1-42. In German, with an abstract in English.

Metcalf RL. 1987. Plant volatiles as insect attractants. Crit Rev Plant Sci 5: 251-301.

Molnár B, Kárpáti Z, Szőcs G, Hall DR. 2009. Identification of female-produced sex pheromone of the honey locust gall midge, *Dasineura gleditchiae*. J Chem Ecol 35: 706-714.

Nachtigall W, Hanauer-Thieser U. 1992. Flight of the honeybee. V. Drag and lift coefficients of the bee's body: implications for flight dynamics. J Comp Physiol B 162: 267-277.

Nichols SW. 1989. The Torre-Bueno glossary of entomology. New York: New York Entomological Society.

Ochieng SA, Park KC, Zhu JW, Baker TC. 2000. Functional morphology of antennal chemoreceptors of the parasitoid *Microplitis croceipes* (Hymenoptera: Braconidae). Arthropod Struct Dev 29: 231-240.

Ochieng SA, Robbins PS, Roelofs WL, Baker TC. 2002. Sex pheromone reception in the scarab beetle *Phyllophaga anxia* (Coleoptera: Scarabaeidae). Ann Entomol Soc Am 95: 97-102.

Porter J, Craven B, Khan RM, Chang SJ, Kang I, Judkewitz B, Volpe J, Settles G, Sobel N. 2007. Mechanisms of scent-tracking in humans. Nat Neurosci 10: 27-29.

Rau P, Rau NL. 1929. The sex attraction and rhythmic periodicity in giant saturniid moths. Trans Acad Sci St Louis 26: 83-221.

Reinecke A, Ruther J, Hilker M. 2002a. The scent of food and defence: green leaf volatiles and toluquinone as sex attractant mediate mate finding in the European cockchafer *Melolontha melolontha*. Ecol Lett 5: 257-263.

Reinecke A, Ruther J, Tolasch T, Francke W, Hilker M. 2002b. Alcoholism in cockchafers: orientation of male *Melolontha melolontha* towards green leaf alcohols. Naturwissenschaften 89: 265-269.

Reinecke A, Ruther J, Hilker M. 2005. Electrophysiological and behavioural responses of *Melolontha melolontha* to saturated and unsaturated aliphatic alcohols. Entomol Exp Appl 115: 33-40.

Reinecke A, Ruther J, Mayer CJ, Hilker M. 2006. Optimized trap lure for male *Melolontha* cockchafers. J Appl Entomol 130: 171-176.

Renou M, Tauban D, Morin JP. 1998. Structure and function of antennal pore plate sensilla of *Oryctes rhinoceros* (L.) (Coleoptera: Dynastidae). Int J Insect Morphol Embryol 27: 227-233.

Roper TJ. 1999. Olfaction in birds. Adv Stud Behav 28: 247-332.

Ruther J, Reinecke A, Thiemann K, Tolasch T, Francke W, Hilker M. 2000. Mate finding in the forest cockchafer, *Melolontha hippocastani*, mediated by volatiles from plants and females. Physiol Entomol 25: 172-179.

Ruther J, Reinecke A, Hilker M. 2002a. Plant volatiles in the sexual communication of *Melolontha hippocastani*: response towards time-dependent bouquets and novel function of (*Z*)-3-hexen-1-ol as a sexual kairomone. Ecol Entomol 27: 76-83.

Ruther J, Reinecke A, Tolasch T, Hilker M. 2002b. Phenol – another cockchafer attractant shared by *Melolontha hippocastani* Fabr. and *M. melolontha* L. Z Naturforsch C 57: 910-913.

Sanes JR, Hildebrand JG. 1976. Structure and development of antennae in a moth, *Manduca sexta*. Dev Biol 51: 282-299.

Schaller D. 1978. Antennal sensory system of *Periplaneta americana* L. Cell Tissue Res 191: 121-139.

Schmidt-Nielsen K. 1997. Animal physiology. 5th ed. Cambridge: Cambridge University Press.

Schneider D, Kaissling KE. 1956. Der Bau der Antenne des Seidenspinners *Bombyx mori* L. I Architektur und Bewegungsapparat der Antenne sowie Struktur der Cuticula. (The construction of the antenna of the silkworm *Bombyx mori* L. I

Architecture and musculoskeletal system of the antenna and the structure of the cuticle.) Zool Jahrb Abt Anat Ontog Tiere 75: 287-310. In German.

Schneider D, Kaissling KE. 1957. Der Bau der Antenne des Seidenspinners *Bombyx mori* L. II Sensillen, cuticulare Bildungen und innerer Bau. (The construction of the antenna of the silkworm *Bombyx mori* L. II Sensilla, cuticular formations and internal construction.) Zool Jahrb Abt Anat Ontog Tiere 76: 223-250. In German.

Schneider D. 1964. Insect antennae. Ann Rev Ent. 9: 103-122.

Schneider RWS, Lanzen J, Moore PA. 1998. Boundary-layer effect on chemical signal movement near the antennae of the sphinx moth, *Manduca sexta*: temporal filters for olfaction. J Comp Physiol A 182: 287-298.

Slifer EH, Sekhon SS. 1961. Fine structure of the sense organs on the antennal flagellum of the honey bee, *Apis mellifera* Linnaeus. J Morph 109: 351-381.

Slifer EH, Sekhon SS, Lees AD. 1964. The sense organs on the antennal flagellum of aphids (Homoptera), with special reference to the plate organs. Quart J Micr Sci 105: 21-29.

Steinbrecht RA. 1970. Zur Morphometrie der Antenne des Seidenspinners, *Bombyx mori* L.: Zahl und Verteilung der Riechsensillen (Insecta, Lepidoptera). (Morphometric studies on the antenna of the silk moth, *Bombyx mori* L.: number and distribution of the olfactory sensilla.) Z Morph Tiere. 68: 93-126. In German, with an abstract in English.

Steinbrecht RA. 1973. Der Feinbau olfaktorischer Sensillen des Seidenspinners (Insecta, Lepidoptera). Rezeptorfortsätze und reizleitender Apparat. (The fine structure of olfactory sensilla in the silk moth [Insecta, Lepidoptera]. Receptor processes and stimulus conduction apparatus.) Z Zellforsch 139: 533-565. In German, with an abstract in English.

Steinbrecht RA. 1984. Chemo-, hygro-, and thermoreceptors. In: Bereiter-Hahn J, Matoltsy AG, Richards, KS, editors. Biology of the integument. Vol. 1. Invertebrates. Berlin: Springer-Verlag. p 523-553.

Steinbrecht RA. 1987. Functional morphology of pheromone-sensitive sensilla. In: Prestwich GD, Blomquist GJ, editors. Pheromone biochemistry. Orlando: Academic Press. p 353-384.

Steinbrecht RA. 1996. Structure and function of insect olfactory sensilla. In: Bock GR, Cardew G, editors. Olfaction in mosquito-host interactions. Ciba Foundation Symposium 200. Chichester: John Wiley & Sons. p 158-177.

Sutton OG. 1949.The science of flight. Harmondsworth: Penguin Books.

Tiemann DL. 1967. Observations on the natural history of the Western banded glowworm *Zarhipis integripennis* (Le Conte) (Coleoptera: Phengodidae). Proc Calif Acad Sci 35: 235-264.

Vareschi E. 1971. Duftunterscheidung bei der Honigbiene – Einzelzell-Ableitungen und Verhaltensreaktionen. (Odour discrimination in the honey bee – single cell and behavioural response.) Z vergl Physiol 75:143-173. In German, with an abstract in English.

Vogel S. 1983. How much air passes through a silkmoth's antenna? 29:597-602.

Vogel S. 1994. Life in moving fluids. 2nd ed. Princeton: Princeton University Press.

Wessel A. 2006. Stridulation in the Coleoptera – an overview. In: Drosopoulos S, Claridge MF, editors. Insect sounds and communication: physiology, behaviour, ecology and evolution. Boca Raton: CRC Press. p 397-403.

Young PG, Beresford-West TBH, Coward SRL, Notarberardino B, Walker B, Abdul-Aziz A. 2008. An efficient approach to converting three-dimensional image data into highly accurate computational models. Phil Trans R Soc A 366: 3155-3173.

Zacharuk RY. 1985. Antennae and sensilla. In: Kerkut GA, Gilbert LI, editors. Comprehensive insect physiology, biochemistry and pharmacology. Vol. 6. Nervous system: sensory. Oxford: Pergamon Press. p 1-69.

Zhang A, Robbins PS, Averill AL, Weber DC, Linn CE, Roelofs WL, Villani MG. 2003. Identification of the female-produced sex pheromone of the scarab beetle, *Hoplia equina*. J Chem Ecol 29: 1635-1642.

FOOTNOTES

[1]We use 'associated with' rather than 'produced by' to allow for the possibility that any pheromone produced by female *Rhipicera* beetles may be associated with other volatile chemicals, e.g. from plants (Metcalf, 1987; Ruther et al., 2000, 2002a; Reinecke et al., 2002a,b, 2005).

[2]In size and shape, the sensilla placodea on the antennae of the male specimen of *R. femorata* most closely resemble the sensilla placodea found on the antennae of bees (Hymenoptera, Apidae; Slifer and Sekhon, 1961, Fig. 7; Fonta and Masson, 1987, Fig. 2) and aphids (Hemiptera, Aphididae; Slifer et al., 1964; Bromley et al., 1979). The sensilla placodea on the antennae of the male specimen of *R. femorata* are, however, morphologically distinct from the sensilla placodea found on the antennae of other beetles, which are smaller, and may be recessed in pits (Meinecke, 1975; Ågren, 1985, Fig. 9; McQuillan and Semmens, 1990, Fig. 5; Renou et al., 1998, Fig. 1; Ochieng et al., 2002, Fig. 1c; Broeckling and Salom, 2003, Fig. 1b; Lu and Wang, 2009, Fig. 6; Bengtsson et al., 2011, Fig. 1). On the other hand, it should be noted that the sensilla placodea of beetle antennae are variable in form (Meinecke, 1975; Renou et al., 1998), and more than one type can be found on the antenna of the same insect (McQuillan and Semmens, 1990, Fig. 5; Leal and Mochizuki, 1993, Fig. 1b).

FIGURE LEGENDS

Fig. 1 (**A**) Male (left) and female (right) specimens of *Rhipicera femorata* used in this study. Short arrow indicates where right antenna of male beetle may have been bent back as a result of becoming entangled with a claw on right foreleg. Long arrow shows where left antenna of female beetle was broken during the course of the scanning electron microscopy. (**B**) Anterior view of male specimen. Boxes: (I) claw on right foreleg entangled in right antenna; (II) instances of light reflected (probably) by flat upper surfaces of sensilla placodea; (III) extraneous particle on antennal surface (highlighted by dashed line). EP: extraneous particle; Gp: gap.

Fig. 2 Models of head and antennae of *Rhipicera femorata*. (**A**) Anterior view of male's left antenna, including part of head. Inset: outline area of antenna. (**B**) Lateral view of male's left antenna. Arrow: presumed direction of airflow through antenna. The faces of the two neighbouring flagellar segments highlighted in blue mark the solid boundaries of an antennal channel. (**C**) Proximal surface of flagellar segment F12 of male's left antenna. (**D**) Posterior edge of flagellar segment F12 of male's left antenna. (**E**) Anterior edges of flagellar segments F12 and F13 of male's left antenna. Inset: length of flagellar segment F12. (**F**) Anterior view of female's right antenna, including part of head. Image reflected for comparison with panel (A). (**G**) Anterior view of flagellar segment F4 of female's right antenna (left) and distal surface of this segment (right). AC: antennal channel; Ba: base of flagellar segment; Bl: blade-like region of flagellar segment; d: distal; *De*: depth of antennal channel; Ey: eye; F*N*: *n*th flagellar segment; Gp: gap; *H*: height of antenna; *L*: length of antenna parallel to presumed direction of airflow; *Le*: length of flagellar segment; *OA*: outline area of antenna (does *not* include scape and pedicel); p: proximal; Pe: pedicel; Sc: scape; St: stem of flagellar segment; *T*: thickness of flagellar segment at its widest point; *w*: width of flagellar segment at its widest point; *W*: width of antenna. Asterisk: 'cut' surface. Red hatched lines: antennal channel.

Fig. 3 (**A**) Male *Rhipicera carinata* beetle on top of wire fence at Spearwood, Perth, Western Australia, 3 April 2014. Arrow indicates probable direction of wind. (**B**) Male *R. carinata* beetle taking off from foliage, Talbot Road Nature Reserve, Stratton, Western Australia, 21 April 2012 (photograph courtesy of Fred and Jean Hort). Note fanned antenna (arrow).

Fig. 4 Silhouettes of (**A**) alert and (**B**) relaxed states of left antenna of male *Rhipicera femorata* beetle. (A) Frontal view of antenna. (B) Dorsal view of antenna. Silhouette in (B) redrawn from Fig. 35, Lawrence and Britton (1994).

Fig. 5 Graphs showing (**A**) length, (**B**) width, (**C**) thickness, and (**E**) surface area of flagellar segments on antennae of *Rhipicera femorata*, together with (**D**) depth of antennal channels. Black and red disks: flagellar segments or antennal channels of left and right antennae, respectively, of male specimen. Yellow and clear squares: flagellar segments or antennal channels of left and right antennae, respectively, of female specimen. Sizes of disks and squares encompass the errors in the data. 'Antennal channel' in (D) refers to the channel formed by two opposing faces of neighbouring flagellar segments (Fig. 2B). E.g. antennal channel 1 is the antennal channel between flagellar segments F1 and F2. See Materials and Methods for explanation of number of flagellar segments/antennal channels represented in each panel.

Fig. 6 Scanning electron micrographs of antennal surface of *Rhipicera femorata*. (**A**) Anterior view of distal portion of male's left antenna. (**B**) Dorsal view of part of female's right antenna. Box labelled 'E' highlights region shown in (E). (**C**) Distal face of flagellar segment F15 of male's right antenna. Small highlighted region on this face is shown in (D); large highlighted region is shown magnified (x 2.3) above flagellar segment. (**D**) Detail of surface of flagellar segment F15 of male's right antenna. (**E**) Detail of surface of flagellar segment F7 of female's right antenna. (**F**) Anterioventral view of male's left antenna. (**G**) Posterior view of male's left antenna. Boxes in (F) and (G): single sensilla placodea. d: Distal; F*N*: *n*th flagellar segment; p: proximal; SB: sensillum basiconicum; SP: sensillum placodeum; ST: sensillum trichodeum.

Fig. 7 Scanning electron micrographs of antennal surface of *Rhipicera carinata*. (**A**) Proximal face of flagellar segment F22 of male's right antenna. (**B**) Dorsal view of part of female's right antenna. Box labelled 'D': region shown in (D). (**C**) Detail of surface of flagellar segment F22 of male's right antenna. (**D**) Detail of surface of

flagellar segment F7 of female's right antenna. FN: Nth flagellar segment; SB: sensillum basiconicum; SP: sensillum placodeum.

VIDEO LEGENDS

Video 1. *Rhipicera carinata* beetles at Spearwood, Perth, Western Australia, 3 April 2014.

Video 2. Model head of male *Rhipicera femorata* beetle.

TABLE 1. Morphometric features of antennae of *Rhipicera femorata*, *Bombyx mori* and *Antheraea polyphemus*

| Morphometric feature[a] | *Rhipicera femorata* | | *Bombyx mori* | *Antheraea polyphemus* |
	Male	Female	Male	Male
Height of antenna (*H*, mm)	5	-	-	8[b]
Width of antenna (*W*, mm)	5-6	4	6[c]	18[b]
Length of antenna parallel to airflow (*L*, mm)	2-3	-	-	3
Outline area of antenna (*OA*, mm^2)	16-17	-	6[d]	117-118
Total surface area of antenna (mm^2)	52-54	5-7	> 86[d]	320-370
Length of flagellar segments (*l*, mm)	0.5-3.3	0.2-0.6	-	-
Width of flagellar segments (*w*, μm)	140-420	140-210	-	-
Thickness of flagellar segments (*T*, μm)	40-240	70-200	-	-
Depth of antennal channels (*De*, μm)	100-490	160-250	-	-
Surface area of flagellar segments (mm^2)	0.3-2.2	0.2-0.3	-	-

[a]All morphometric features except for the total antennal surface area and the surface area of the flagellar segments are defined in Fig. 2; [b]Boeckh et al. (1960, Table 1) - these figures agree with those obtained from our models of the antennae of *A. polyphemus*; [c]estimated from Fig. 2b of Steinbrecht (1970); [d]Steinbrecht (1970, Table 3) - the figure given (> 86 mm^2) for the total antennal surface area is the sum of the non-sensory antennal surface area (> 75 mm^2) and the total surface area of the pheromone-receptive sensilla trichodea (11 mm^2).

TABLE 2. Physical characteristics of antennae of male *Rhipicera femorata* beetle

Physical characteristic	Value
Reynolds numbers of whole antennae	100 – 1,000
Reynolds numbers of antennal channels	10 – 200
Diffusion times in antennal channels (ms)	0.5 – 10

TABLE 3. Number and density of sensilla placodea on antennae of male *Rhipicera femorata* beetle

Flagellar segment	Number of sensilla placodea				Density of sensilla placodea (mm^{-2})			
	Left		Right		Left		Right	
	Inner face	Outer face	Inner face	Outer face	Inner face	Outer face	Inner face	Outer face
1	56	-	-	-	171	-	-	-
3	-	111	-	-	-	295	-	-
7	-	593	-	-	-	665	-	-
9	-	564	-	-	-	557	-	-
13	-	699	-	-	-	650	-	-
14	-	663	-	-	-	616	-	-
15	-	660	-	641	-	622	-	613
16	-	621	689	-	-	591	645	-
25	522	-	517	-	651	-	652	-
26	469	-	481	-	656	-	648	-
27	418	-	-	-	616	-	-	-
28	372	-	397	-	595	-	648	-
29	338	-	348	-	599	-	616	-
30	292	-	-	-	568	-	-	-
31	259	-	286	-	578	-	644	-
32	217	-	261	-	536	-	651	-
33	175	-	189	-	520	-	577	-
34	147	-	148	-	519	-	570	-
35	101	-	89	-	493	-	503	-
36	75	-	54	-	414	-	399	-

TABLE 4. Total number of sensilla (placodea or pheromone-receptive trichodea) on single male antennae of *Rhipicera femorata, Bombyx mori* and *Antheraea polyphemus*

	Rhipicera femorata	*Bombyx mori*	*Antheraea polyphemus*
Number of sensilla	30,000[a]	17,000[b]	55,000[c]

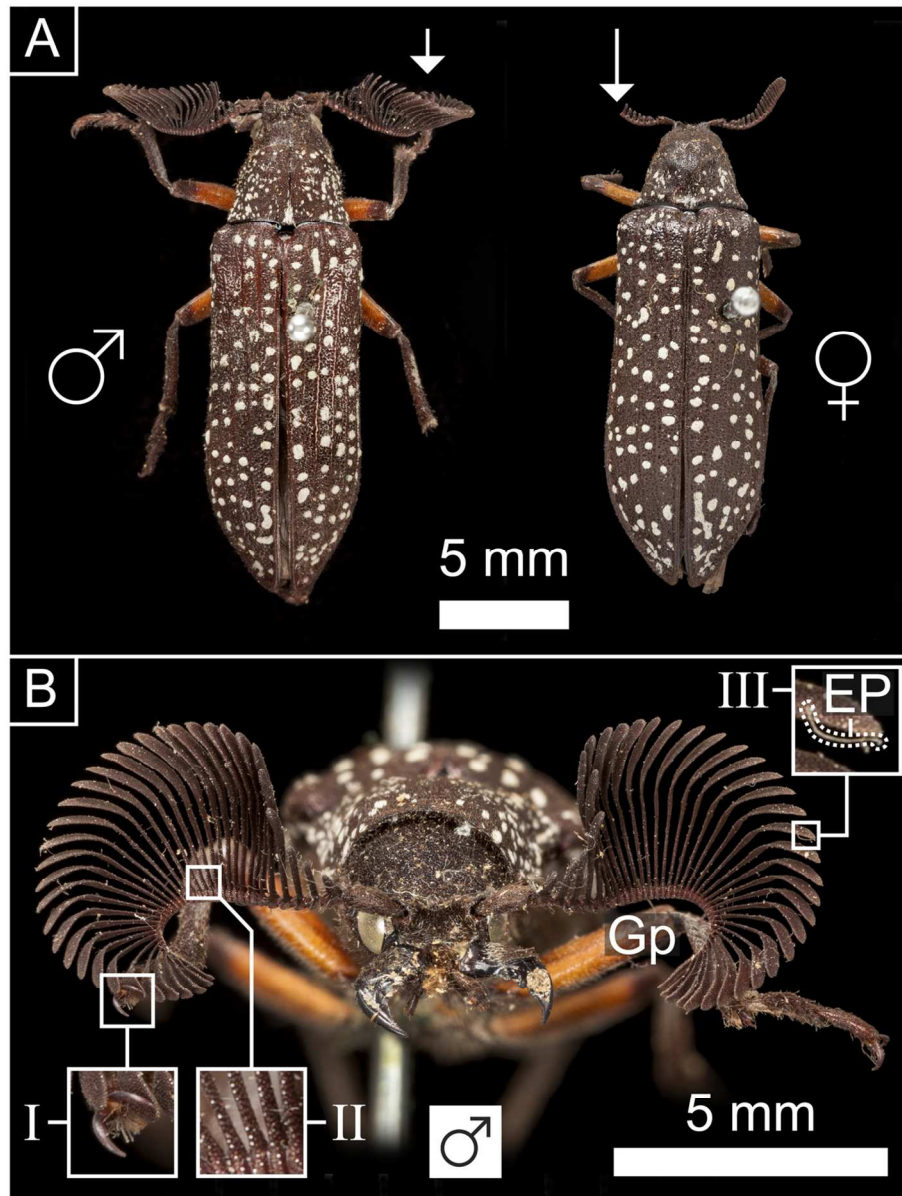[a]Estimate from current study; [b]Steinbrecht (1970, Table 3); [c]Boeckh et al. (1960, Table 2).

Fig. 1 (A) Male (left) and female (right) specimens of *Rhipicera femorata* used in this study. Short arrow indicates where right antenna of male beetle may have been bent back as a result of becoming entangled with a claw on right foreleg. Long arrow shows where left antenna of female beetle was broken during the course of the scanning electron microscopy. (B) Anterior view of male specimen. Boxes: (I) claw on right foreleg entangled in right antenna; (II) instances of light reflected (probably) by flat upper surfaces of sensilla placodea; (III) extraneous particle on antennal surface (highlighted by dashed line). EP: extraneous particle; Gp: gap.
112x148mm (300 x 300 DPI)

Fig. 2 Models of head and antennae of *Rhipicera femorata*. (A) Anterior view of male's left antenna, including part of head. Inset: outline area of antenna. (B) Lateral view of male's left antenna. Arrow: presumed direction of airflow through antenna. The faces of the two neighbouring flagellar segments highlighted in blue mark the solid boundaries of an antennal channel. (C) Proximal surface of flagellar segment F12 of male's left antenna. (D) Posterior edge of flagellar segment F12 of male's left antenna. (E) Anterior edges of flagellar segments F12 and F13 of male's left antenna. Inset: length of flagellar segment F12. (F) Anterior view of female's right antenna, including part of head. Image reflected for comparison with panel (A). (G) Anterior view of flagellar segment F4 of female's right antenna (left) and distal surface of this segment (right). AC: antennal channel; Ba: base of flagellar segment; Bl: blade-like region of flagellar segment; d: distal; De: depth of antennal channel; Ey: eye; F*N*: *n*th flagellar segment; Gp: gap; *H*: height of antenna; *L*: length of antenna parallel to presumed direction of airflow; *Le*: length of flagellar segment; *OA*: outline area of antenna (does *not* include scape and pedicel); p: proximal; Pe: pedicel; Sc: scape; St: stem of flagellar segment; *T*: thickness of flagellar segment at its widest point; *w*: width of flagellar segment at its widest

point; *W*: width of antenna. Asterisk: 'cut' surface. Red hatched lines: antennal channel.
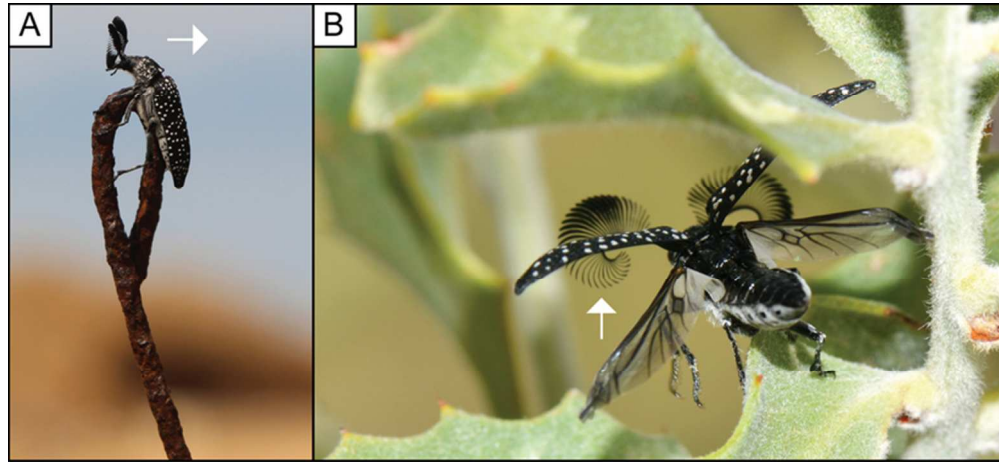183x222mm (300 x 300 DPI)

Fig. 3 (A) Male *Rhipicera carinata* beetle on top of wire fence at Spearwood, Perth, Western Australia, 3 April 2014. Arrow indicates probable direction of wind. (B) Male *R. carinata* beetle taking off from foliage, Talbot Road Nature Reserve, Stratton, Western Australia, 21 April 2012 (photograph courtesy of Fred and Jean Hort). Note fanned antenna (arrow).
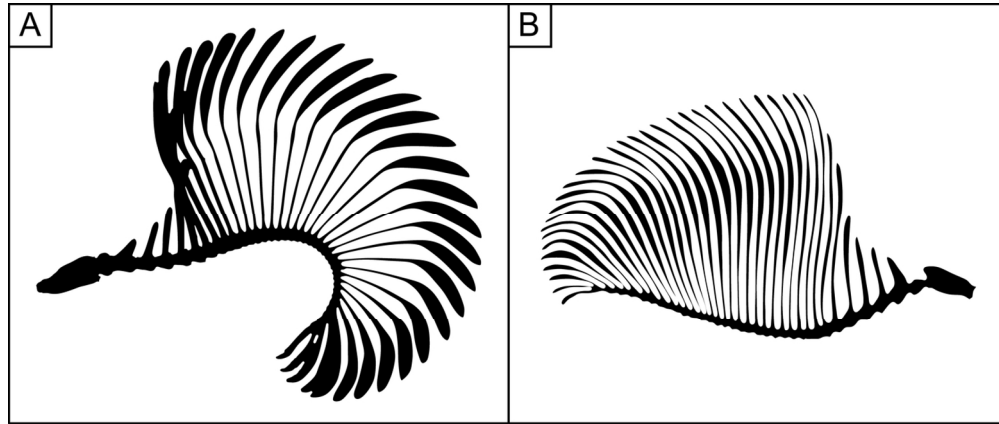69x31mm (300 x 300 DPI)

Fig. 4 Silhouettes of (A) alert and (B) relaxed states of left antenna of male *Rhipicera femorata* beetle. (A) Frontal view of antenna. (B) Dorsal view of antenna. Silhouette in (B) redrawn from Fig. 35, Lawrence and Britton (1994).
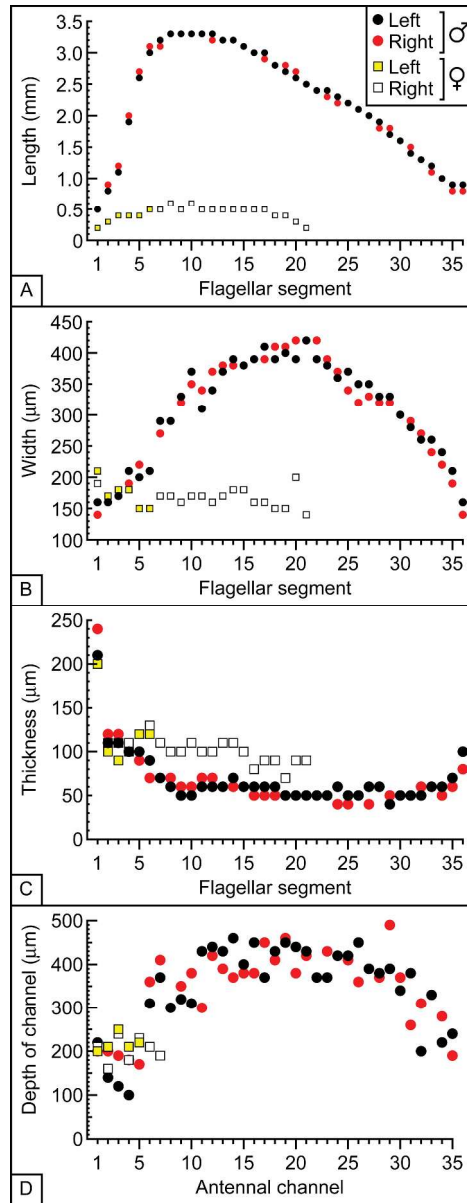63x26mm (600 x 600 DPI)

Fig. 5 Graphs showing (A) length, (B) width, (C) thickness, and (E) surface area of flagellar segments on antennae of *Rhipicera femorata*, together with (D) depth of antennal channels. Black and red disks: flagellar segments or antennal channels of left and right antennae, respectively, of male specimen. Yellow and clear squares: flagellar segments or antennal channels of left and right antennae, respectively, of female specimen. Sizes of disks and squares encompass the errors in the data. 'Antennal channel' in (D) refers to the channel formed by two opposing faces of neighbouring flagellar segments (Fig. 2B). E.g. antennal channel 1 is the antennal channel between flagellar segments F1 and F2. See Materials and Methods for explanation of number of flagellar segments/antennal channels represented in each panel.
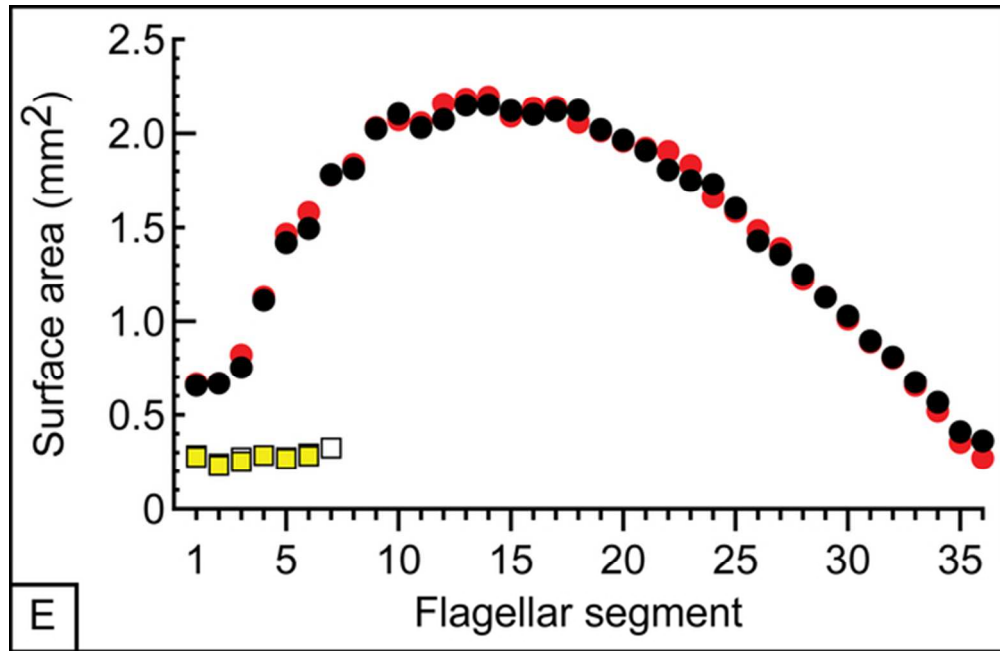220x568mm (300 x 300 DPI)

Fig. 5 Graphs showing (A) length, (B) width, (C) thickness, and (E) surface area of flagellar segments on antennae of *Rhipicera femorata*, together with (D) depth of antennal channels. Black and red disks: flagellar segments or antennal channels of left and right antennae, respectively, of male specimen. Yellow and clear squares: flagellar segments or antennal channels of left and right antennae, respectively, of female specimen. Sizes of disks and squares encompass the errors in the data. 'Antennal channel' in (D) refers to the channel formed by two opposing faces of neighbouring flagellar segments (Fig. 2B). E.g. antennal channel 1 is the antennal channel between flagellar segments F1 and F2. See Materials and Methods for explanation of number of flagellar segments/antennal channels represented in each panel.
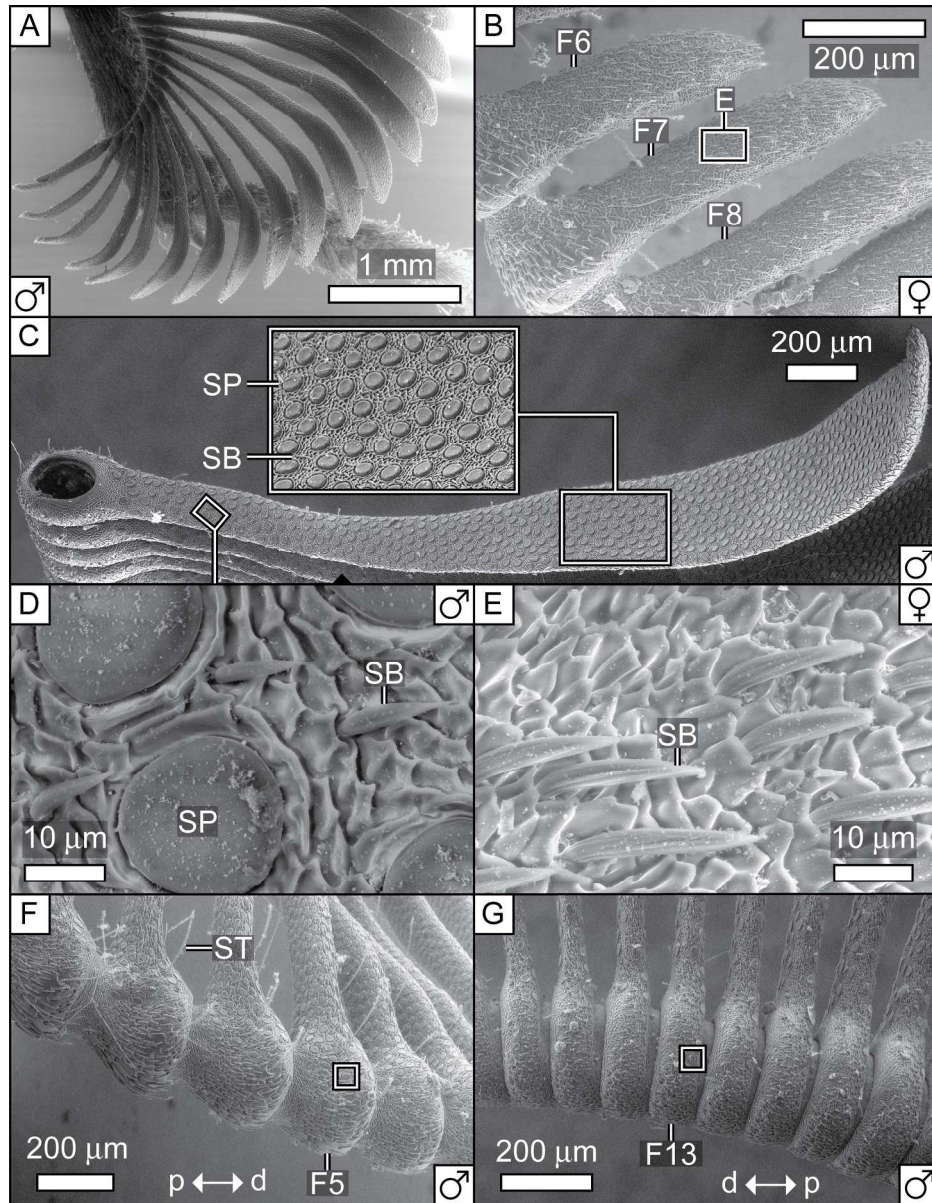55x35mm (300 x 300 DPI)

Fig. 6 Scanning electron micrographs of antennal surface of *Rhipicera femorata*. (A) Anterior view of distal portion of male's left antenna. (B) Dorsal view of part of female's right antenna. Box labelled 'E' highlights region shown in (E). (C) Distal face of flagellar segment F15 of male's right antenna. Small highlighted region on this face is shown in (D); large highlighted region is shown magnified (x 2.3) above flagellar segment. (D) Detail of surface of flagellar segment F15 of male's right antenna. (E) Detail of surface of flagellar segment F7 of female's right antenna. (F) Anterioventral view of male's left antenna. (G) Posterior view of male's left antenna. Boxes in (F) and (G): single sensilla placodea. d: Distal; F*N*: *n*th flagellar segment; p: proximal; SB: sensillum basiconicum; SP: sensillum placodeum; ST: sensillum trichodeum. 194x251mm (300 x 300 DPI)
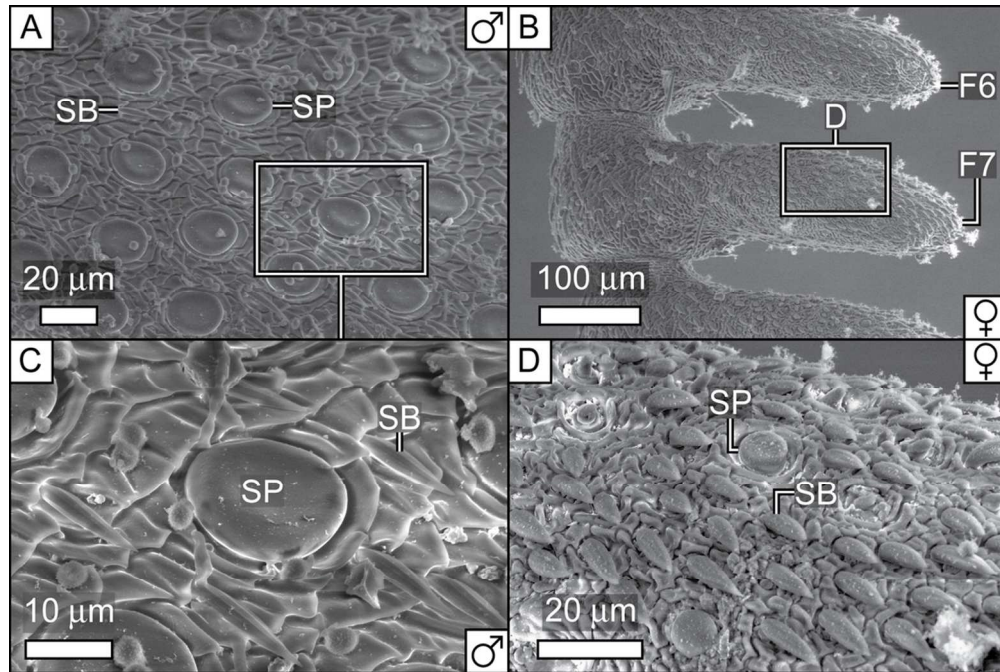
Fig. 7 Scanning electron micrographs of antennal surface of *Rhipicera carinata*. (A) Proximal face of flagellar segment F22 of male's right antenna. (B) Dorsal view of part of female's right antenna. Box labelled 'D': region shown in (D). (C) Detail of surface of flagellar segment F22 of male's right antenna. (D) Detail of surface of flagellar segment F7 of female's right antenna. F*N*: *N*th flagellar segment; SB: sensillum basiconicum; SP: sensillum placodeum.
100x66mm (300 x 300 DPI)